Thermal Annealing induced phase transition and UV Irradiation Induced brightening in CdS nanoparticles

M. A. Osman[1], A. A. Othman[1] and A. G. Abed-Elrahim[1]

[1] *Physics department, Faculty of Science, Assiut University*

Abstract

CdS nanoparticles were synthesized by aqueous co-precipitation method. Samples were annealed in air for 3 hrs in the temperature range 200-700 °C to study the effect of annealing temperature (T_a) on structural, morphological and optical properties of CdS nanoparticles. CdS nanoparticles dispersed in double distilled water was UV irradiated to investigate photo-induced changes in the optical absorption edge. Structural, morphological and optical properties were characterized using XRD, HRTEM and UV-vis absorption. The increase in the average crystallite size D from 3 to 23 nm as a result of thermal annealing has been estimated from XRD. Observed phase transitions occurred at T_a = 300 ^oC from as prepared Cubic to hexagonal CdS structure and from hexagonal CdS at T_a = 500 ^oC to $CdSO_3$ monoclinic structure at T_a = 600 ^oC. Analysis of UV-vis absorption spectra, show remarkable decrease in optical band gap (E_g^{opt}) from 3.4 for as prepared to 2.5 eV at 500 ^oC with increasing T_a, as a result, in crystallinity enhancement and increase in particle size, which in turn leads to the reduction of quantum confinement. UV induced effect on CdS nanoparticles leads to an enhancement in the optical transmittance T% accompanied with increase in the optical band gap E_g^{opt} (i.e. photo brightening). The photo brightening can be explained in terms of an induced photolysis by photo-ionization, results, in corrosion of CdS nanoparticles, which in turns leads to reduction in particle size (E_g^{opt} increasing).

Keywords: CdS nanoparticles, phase transition, optical absorption, thermal annealing, UV induced photo-brightening.

1. Introduction

Semiconductor nanomaterials are promising materials for many fields of research, due to the size dependant tunability of their physical and chemical properties. Bulk CdS semiconductor posses stable hexagonal structure and optical band gap = 2.42 eV[1]. Due to the quantum size effect, CdS nanostructures has novel physical and chemical properties which show significant difference from their bulk, when the length scale is comparable to the exciton Bohr radius [2–4]. These size dependent novel characteristics of CdS nanostructures makes it promising material for many applications such as highly efficient photo catalysis [5], cell imaging [6], solar photovoltaic cells [7], field effect transistors [8], light emitting diodes[9 ,10] and biomedical application[11]. Many studies have been carried out under different Circumstances such capping, doping type or preparation technique to investigate the size dependant properties [12–14]. The present study aims to investigate thermal annealing effects on structural, morphological and optical properties, in addition to UV irradiation induced effect on optical absorption edge of CdS nanoparticles.

2. Experimental details

2.1. Sample Preparation

CdS nanoparticles were synthesized at room temperature using chemical precipitation method. Cadmium acetate ($Cd(CH_3COO)_2$), sodium sulfide (Na_2S) were used as source materials, and EDTA

($C_{10}H_{16}N_2O_8$) as a Capping agent. All chemicals used were of AR grade. 0.8M $Cd(CH3COO)_2.2H_2o$ was dissolved in 75 ml double distilled water, 0.08 M EDTA was added to solution of Cd^{+2} ions and o.8 M of Na_2S was dissolved in 75 ml double distilled water and added drop wise with constant stirring at 400 rpm. The obtained fine orange precipitate was filtered out and washed several times with distilled water and ethanol to remove unnecessary impurities formed during the preparation process. CdS samples were dried at 100 ^oC for 3 hrs to remove moisture. To study the effect of annealing process on morphological, structural and optical properties, the samples of CdS were annealed in the temperature range 200–700 ^oC in atmospheric air with the step of 100 ^oC, then the samples were cooled to room temperature at the rate of 10 °C/min.

2.2. Characterization

The Crystal structure of CdS nanoparticles samples was characterized by X-ray diffraction (PW 1700 X-ray diffractometer with Cu Kα radiation λ=1.54056Å), diffraction patterns were recorded in the range of the diffraction angle 2**θ** from/20 to 70^o, with a step of 0.06°. UV-vis optical absorption spectra were studied using Perkin Elmer lambda 750 spectrophotometer at room temperature. Fourier transform infrared spectroscopy (FTIR) [Nicolet™ iS™10 FT-IR Spectrometer] was used to identify the functional groups in the samples. Particle size, morphology and crystalline nature were investigated by using high resolution transmission electron microscope (HRTEM) [Jeol Jem 2100 microscope operating at 200 kV]. Photo induced effect was investigated by using mercury lamp [VL-6.LC] at λ =254nm and power of 6 watt.

3. Results and discussion

3.1. XRD analysis

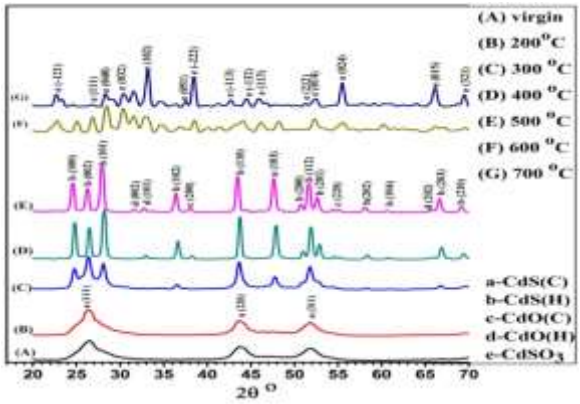

Fig.1 XRD patterns of the CdS nanoparticles at different annealing temperatures

Fig.1 show XRD patterns for as prepared CdS nanoparticles and annealed samples at different annealing temperatures in the range from 200 ^oC to 700 ^oC. For as prepared sample there are Three prominent peaks at 2θ = 26.48^o, 43.7^o and 51.8^o matching with CdS cubic structure [JCPDS:04-006-3897] with no secondary peaks of any impurities. From the width of the XRD peaks broadening which reflect the nanocrystalline nature**,** crystallite size (D) was determined using scherer equation [15]:

$$D = \frac{K\lambda}{\beta \cos\theta} \quad (1)$$

Where K(particle shape factor) ≅ 0.9, λ (x-ray wavelength) = 0.154 nm, β is the full width at half-maximum (FWHM) and θ is the diffraction angle. Crystallite size (D) of as prepared and annealed samples up to T_a= 500^{o}C were calculated according to the above equation and recorded in table 1(a). The observed Increase in D from 3nm for as prepared CdS to 17.6 nm for annealed sample at 500 ^{o}C can be explained as reaction of residual

source during the annealing process, and agglomeration tendency behavior of nanoparticles [16]. Structural transformation from as prepared cubic to hexagonal structure of CdS at T_a= 300 ^oC was observed and its indexed planes were in a good match with standard [JCPDS:01-075-1545]. This structural transformation can be interpreted as a result of size driven structural transformation by annealing process and these results are in agreement with those reported by Bandaranayake et.al [17]. Further annealing up to T_a = 500 ^oC leads to sharper XRD peaks, hence enhancement of crystallinity. In addition, traces of CdO phases which indexed in XRD planes matching with standard [JCPDS:04-016-6730], represent oxidation process starting at the same temperature. Increase in annealing temperature up to 600 ^oC and 700 ^oC, results in further oxidation and evolution of another structural transformation from CdS hexagonal structure to $CdSO_3$ monoclinic structure and the indexed planes for this structure is in agreement with standard cards [JCPDS:04-012-3174 and 00-037-0001].

3.2. Optical analysis

3.2.1. Annealing effects

Annealing effects on optical properties of CdS nanoparticles were studied using Tauc analysis [fig. 2(a)], according to the following equation [18]:

$$(\alpha h\nu) = B\,(h\nu - E_g^{opt})^{n} \quad (2)$$

Where $\mathbf{n = 1/2}$ for the direct allowed transition, α is the absorption coefficient, hv is the photon energy and B is the steepness parameter. Small size of nanoparticles results, in spatial confinement of the charge carrier wave functions, which is termed as quantum size effect, consequently size reduction for as prepared CdS (D = 3 nm), which is comparable to exciton Bohr radius [19], results in a blue shift in optical band gap for as prepared CdS nanoparticles E_g^{opt}(nano) = 3.4 eV which is larger than the corresponding bulk value E_g^{opt} (bulk) = 2.42 eV [1]. Raising annealing temperature leads to observable decrease in E_g^{opt} accompanied with reduction of transmittance T% [inset of fig. 2(a)].

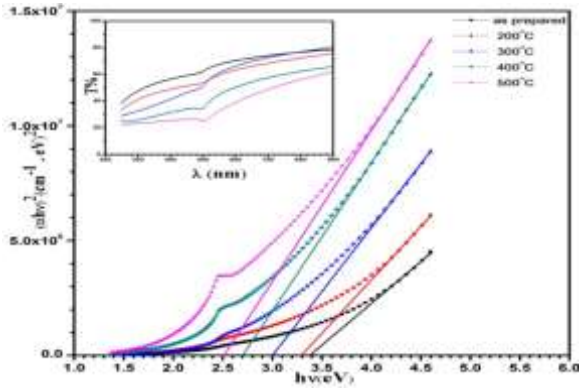

Fig. 2(a) $(\alpha h\nu)^2$ vs. hv of CdS nanoparticles at annealing different temperatures and T% vs. λ on the inset

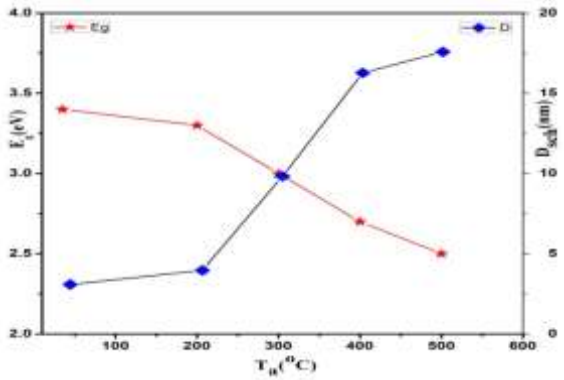

Fig. 2(b) dependence of both E_g^{opt} and D on annealing temperature T_a

Fig. 2(b) shows the annealing effect on both optical band gap and crystallite size. It is noticed that increasing in T_a up to 500 ^oC, results in decrease E_g^{opt} from 3.4 eV for as prepared to 2.5 eV for sample annealed at 500 ^oC. This reduction of optical band gap can be explained as a result to overlapping weaken of electron and hole wave

functions, which result from reduction of quantum size effect and enhancement of crystallinity accompanied with increase of particle size.

3.2.2. UV induced effects

Fig. 3(a) shows Tauc analysis for optical absorption of CdS nanoparticles dispersed in double distilled water, which irradiated by UV for different irradiation times in the range from 0 to 120 minute to investigate the photo induced effects on the optical absorption edge. The Increase in UV irradiation times results, in enhancement of transmittance spectrum (photo-bleaching) [inset of fig. 3(a)], accompanied by increasing E_g^{opt}. This behavior can be explained in terms of two stage process stimulated by optical excitation:(a) photoionization which occur essentially due to Auger process, in which one electron – hole pair recombine providing an extra electron energy to leave the crystallite.(b) stimulated photolysis providng an irreversible paricles corrosion i.e. reduction of particle size, which leads to stronger overlap between electron and hole wave function, hence enhancement of transmittance[20].

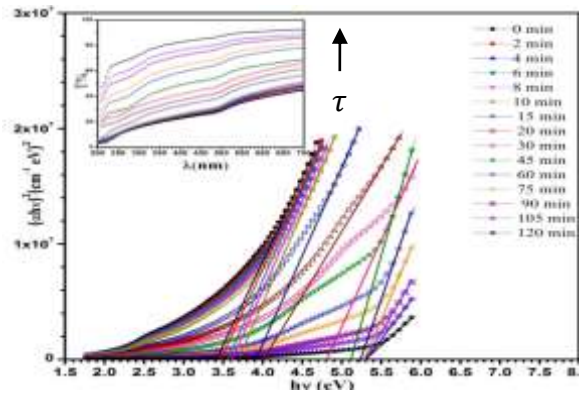

Fig. 3(a) $(\alpha h\nu)^2$ vs. hν of CdS nanoparticles at different UV irradiation times τ and T% vs. λ on the inset

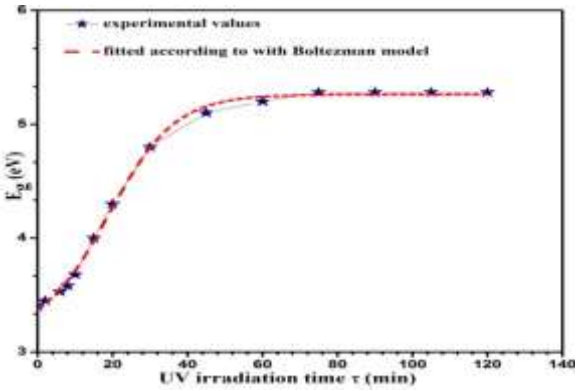

Fig. 3(b) dependence of E_g^{opt} on UV irradiation time τ

Photoionization induces sequence of chemical reactions by means of Auger process yield an excess electron outside the crystallite and an excess hole inside or at the surface that is can be expressed as follow [21]:

$$(CdS)_n \xrightarrow{h\nu} (CdS)_n(e^- + h^+) \xrightarrow{h\nu} (CdS)_n(e^- + h^+)_2 \longrightarrow (CdS)_n(h^+) + e^- . \quad (3)$$

After photoionization, the remaining hole may act an oxdizing agent and intiate the secondary chemical reactions at the CdS surface i.e. photo passivation. Sulfide anions can be oxidized to the radical anion S^- by h^+ with further oxidation by air oxygen SO_2^- or SO_4^- that is ,

$$h^+ + S^{-2} \longrightarrow S^- \quad , \quad S^- + O_2 \longrightarrow SO_2^- \xrightarrow{O2} SO_4^{-2} \quad (4)$$

Such anions have been detected after photolysis of CdS nanoparticles colloidal solution by Kamat [22]. Fig. 3(b) shows the dependence of E_g^{opt} on UV irradiation times (τ) which obey an empirical equation in a good agreement with Boltzmann fitting for our data, with adjusting $R^2 = 0.998$ as follow:

$$\mathbf{E_g^{opt}} = \mathbf{5.26} - \frac{\mathbf{2.106}}{\boldsymbol{e}^{\left(\frac{\tau - 18.975}{8.81}\right)}} \quad (\mathbf{5})$$

It is observed that two characteristic regions of E_g^{opt} dependence on UV irradiation time $\boldsymbol{\tau}$. First region from the start of UV exposing up to nearly 40 minute, the second from 40 minute up to 120 minute. We suggest that in the first region, photolysis stimulated by photo ionization of nanoparticles is more prominent, consequently rapid decrease in the corresponding dispersed particle size and enhancement of quantum size effect that leads to increasing of optical band gap. Second region photo-oxidation is the most prominent, results in photo-passivation on the surface of nanoparticles, consequently, consequently stability of particle size value, which reflect the saturation in E_g^{opt} with irradiation time at higher dose.

3.3. Morphology and HRTEM studies

Figs. 4(a,b,c,d) show TEM images for as prepared CdS nanoparticles and annealed samples at T_a= 300 ^oC, 500 ^oC and 600 ^oC. TEM Image for as prepared CdS, showed that it mostly a monodispersed spherical shape with narrow size distribution, (where standard dev. $\approx \mathbf{1.9}$< 7%), and the average particle size D$\approx$ $\mathbf{6.25\ nm}$, calculated from the corresponding histogram. From TEM Images (b) T_a = 300 ^oC, (c) T_a = 500 ^oC, (d) Ta = 600 ^oC, it is clear that increasing in annealing temperature leads to the growth and agglomeration of small particles to form larger average particle size [table 1(a)], furthermore, morphology modification from a monodispersed spherical shape for as prepared CdS nanoparticles to a wide distribution of large grains, mixed spherical and hexagonal shapes for the sample annealed at T_a = 500 ^oC and 600 ^oC.

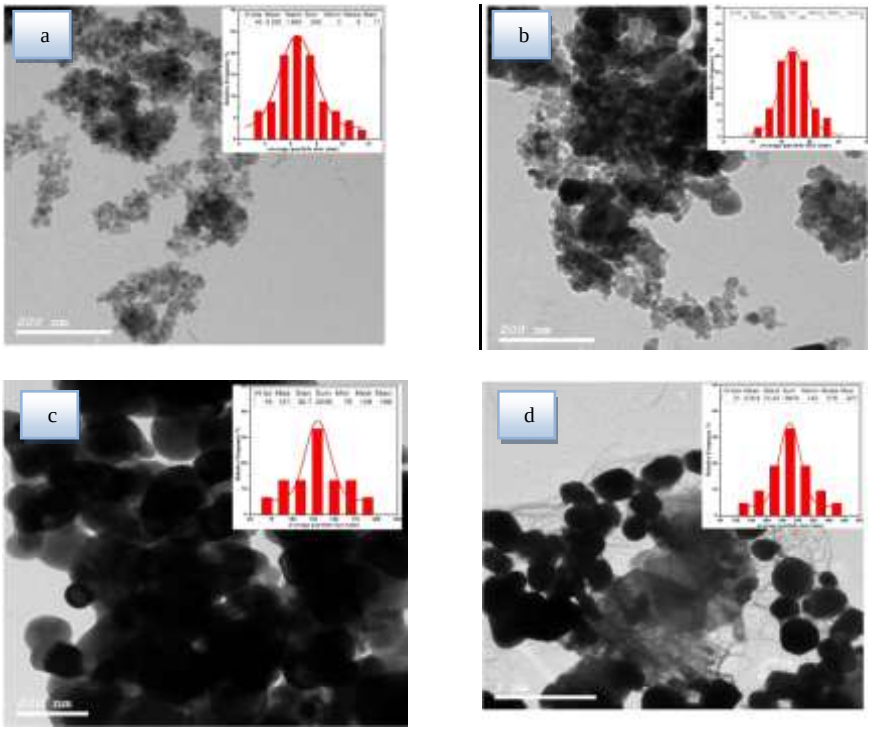

Figs. 4 TEM images for (a) as prepared, (b) 300 ^oC, (c) 500 ^oC, (d) 600^oC and the corresponding histogram on the inset of CdS nanoparticles

Lattice parameters of the as prepared CdS nanoparticles and annealed samples was investigated via analysis of both HRTEM and SAED [figs. 5(a,b,c,d)]. HRTEM and the corresponding SAED for the as prepared CdS cubic structure [fig. 5(a)], reveals the polycrystalline nature with a preferable orientation indexed by miller indices (111), (220) and (311). The measured interplanar distances d_{hkl} determined from HRTEM, SAED and XRD as well as, the calculated lattice parameters (table 1(a)), are in a good agreement with each other and with the standard card [JCPDS:04-006-3897]. Increase in annealing temperature up to 500 ^oC leads to an

enhancement in crystallinity, manifested in increasing domain boundaries as a result of defects reduction and appearance of intense bright spots on the diffraction rings (inset of fig. 5(c)). Further increase in annealing temperature up 600 ^{o}C and 700 ^{o}C leads to the oxidation of CdS to CdSO3, which interplanar distances d_{hkl} determined from HRTEM, SAED and XRD and the calculated lattice parameter (table 2(a)), are in good agreement with standard cards [JCPDS:04-012-3174 and 00-037-0001].

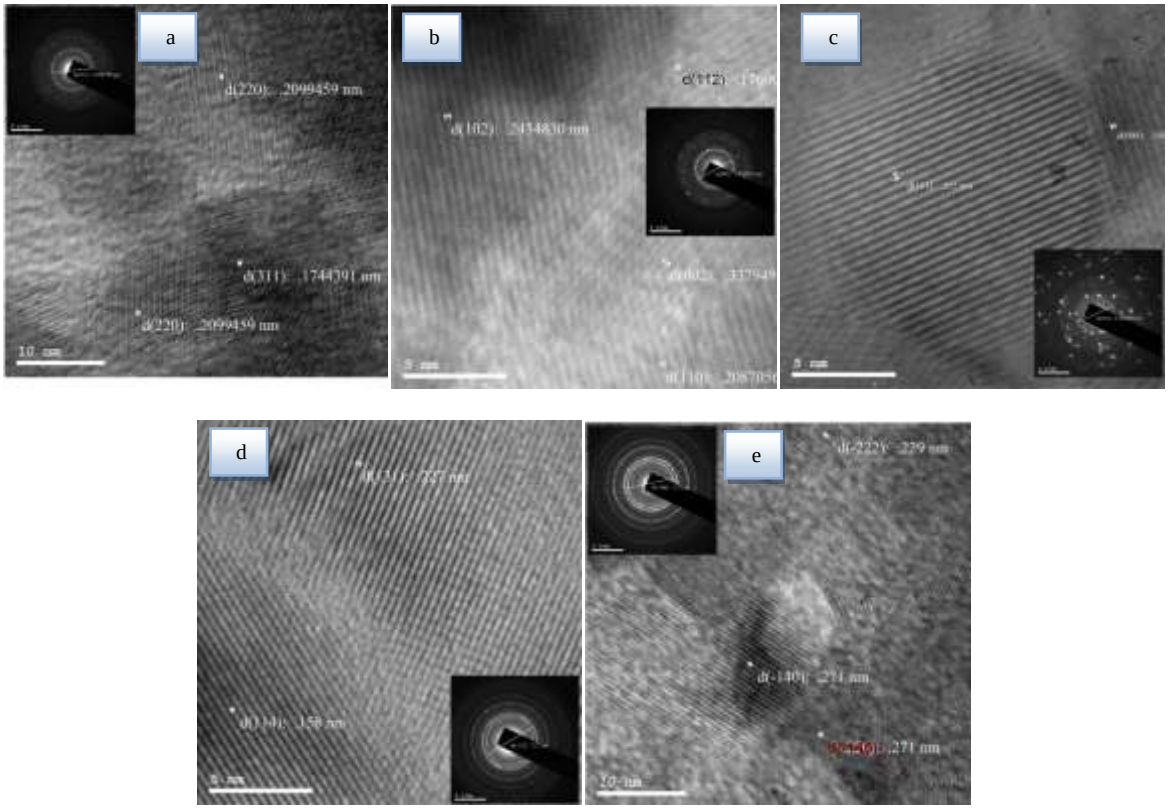

Figs. 5 HRTEM images for (a) as prepared, (b) 300 ^{o}C, (c) 500 ^{o}C, (d) 600 ^{o}C and (e) 700 ^{o}C of CdS nanoparticles and the corresponding SAED on the inset.

4. Conclusions

a) Monodisperse CdS nanocrystallites with D ≈ $3nm$ and E_g^{opt} =3.4 eV were prepared by co-precipitation method.

b) Thermal annealing results in, the increase in the crystallite size D from =3 nm to 23 nm, accompanied by decrease of optical band gap E_g^{opt} from 3.4 eV to 2.5 eV as a result of reduction of quantum size effect.

c) Structure phase transitions was observed from as prepared cubic to hexagonal CdS structure at T_a=300 ^{o}C and from hexagonal CdS to monoclinic $CdSO_3$ structure starts at T_a = 600 ^{o}C.

d) HRTEM images as well as, SAED patterns, show polycrystalline nature for the as prepared CdS and crystallinity enhancement by increasing annealing temperature up to T_a = 500 ^{o}C.

e) UV irradiation of colloidal solution of CdS nanoparticles leads to an enhancement in transmittance accompanied by increase in the optical band gap as a result of photolysis stimulated by photo ionization.

f) Thermal annealing and UV induced effects serve as powerful tools for size tuning, hence, controlling size dependent physical and chemical properties.

Table 1(a): Dependence of D, E_g^{opt}, d_{hkl} and lattice parameters of CdS nanoparticles on T_a up to = 500 °C

T_a (°C)	Phase	Average particle size D(nm)		Eg (eV)	Lattice parameters (Å)								
					Interplanar distance d_{hkl}					Average lattice constant a, b and c			
		XRD	TEM		hkl	XRD	HRTEM	SAED	Ref. card	XRD	HRTEM	SAED	Ref. card
virgin	CdS (c)	3.08	6.28	3.4	(111)	3.363		3.36	3.366	a=b=c= 5.842	a=b=c= 5.81	a=b=c= 5.9	a=b=c= 5.83
					(220)	2.07	2.1	2.09	2.061				
					(311)	1.763	1.74	1.8	1.757				
300	CdS (H)	9.83	16.6	3	(002)	3.39	3.38	3.377	3.37	a=b=4.16 c=6.78	a=b=4.1 c=6.76	a=b=4.11 c=6.754	a=b=4.15 c=6.737
					(102)	2.47	2.45	2.45	2.46				
					(110)	2.08	2.08	2.06	2.07				
					(112)	1.76	1.761	1.76	1.766				
500	CdS (H)	17.58	127.25	2.5	(101)	3.19	3.15	3.173	3.17	a=b=4.18 c=6.748	a=b=4.11 c=6.76	a=b=4.15 c=6.742	a=b=4.15 c=6.737
					(004)	1.687	1.69	1.68	1.684				
					(211)	1.331		1.331	1.331				
					(105)	1.26		1.26	1.263				
	CdO (C)				(200)	2.36		2.34	2.347	a=b=c= 4.72		a=b=c= 4.68	a=b=c= 4.695

Table 1(b): Dependence of D, d_{hkl} and lattice parameters of $CdSO_3$, result from annealing of CdS nanoparticles at T_a = 600 °C, 700 °C

Ta (°C)	Phase	Average particle size D(nm)		Lattice parameters (Å)								
				Interplanar distance dhkl					Average lattice constant a, b and c			
		XRD	TEM	hkl	XRD	HRTEM	SAED	Ref. card	XRD	HRTEM	SAED	Ref. card
600	CdSO3 (Monoclinic)	8.4	280	(-112)	2.714		2.75	2.746	a = 4.12 , b = 9.03, c = 7.12 β = 96.68°	—	a = 4.4, b = 8.544, c = 7.2 β = 94.69°	a = 4.44 , b = 8.61, c = 7.18 β = 94.53 °
				(131)	2.247	2.27	2.238	2.239				
				(114)	1.536	1.58	1.587	1.588				
				(025)	1.350		1.360	1.358				
				(-135)	1.120		1.1257	1.1254				
				(-112)	2.714		2.750	2.746				
700		23		(-140)	2.699	2.71	2.720	2.720	—	—	—	—
				(-222)	2.339	2.29	2.340	2.317				
				(250)	1.352		1.380	1.358				
				(253)	1.152		1.162	1.157				

References

[1] D. C. Onwudiwe and P. a Ajibade, "ZnS, CdS and HgS nanoparticles via alkyl-phenyl dithiocarbamate complexes as single source precursors.," *Int. J. Mol. Sci.*, vol. 12, no. 9, pp. 5538–51, Jan. 2011.

[2] R. Banerjee, R. Jayakrishnan, and P. Ayyub, "Effect of the size-induced structural transformation on the band gap in CdS nanoparticles," vol. 12, pp. 10647–10654, 2000.

[3] Y. Azizian-kalandaragh and A. Khodayari, "Effect of thermal annealing and gamma irradiation on the optical properties of CdS-polymer nanocomposites," vol. 4, no. 6, pp. 881–883, 2010.

[4] W. M. De Azevedo and F. D. Menezes, "A new and straightforward synthesis route for preparing Cds quantum Dots," *J. Lumin.*, vol. 132, no. 7, pp. 1740–1743, 2012.

[5] S. Cao, C.-J. Wang, X.-J. Lv, Y. Chen, and W.-F. Fu, "A highly efficient photocatalytic H2 evolution system using colloidal CdS nanorods and nickel nanoparticles in water under visible light irradiation," *Appl. Catal. B Environ.*, vol. 162, no. 0, pp. 381–391, Jan. 2015.

[6] Y. Bao, J. Li, Y. Wang, L. Yu, J. Wang, W. Du, L. Lou, Z. Zhu, H. Peng, and J. Zhu, "Preparation of water soluble CdSe and CdSe/CdS quantum dots and their uses in imaging of cell and blood capillary," *Opt. Mater. (Amst).*, vol. 34, no. 9, pp. 1588–1592, Jul. 2012.

[7] Y. Kashiwaba, K. Isojima, and K. Ohta, "Improvement in the efficiency of Cu-doped CdS / non-doped CdS photovoltaic cells fabricated by an all-vacuum process," vol. 75, pp. 253–259, 2003.

[8] B. Mereu, G. Sarau, E. Pentia, V. Draghici, M. Lisca, T. Botila, and L. Pintilie, "Field-effect transistor based on nanometric thin CdS films," *Mater. Sci. Eng. B*, vol. 109, no. 1–3, pp. 260–263, Jun. 2004.

[9] J.-U. Kim, Y.-S. Kim, and H. Yang, "Nanocrystalline Y3Al5O12:Ce phosphor-based white light-emitting diodes embedded with CdS:Mn/ZnS core/shell quantum dots," *Mater. Lett.*, vol. 63, no. 6–7, pp. 614–616, Mar. 2009.

[10]Y. Lin, Y. Zhang, J. Zhao, P. Gu, K. Bi, Q. Zhang, H. Chu, T. Zhang, T. Cui, Y. Wang, J. Zhao, and W. W. Yu, "White-light-emitting diodes using GaN-excited CdSe/CdS/ZnS quantum dots," *Particuology*, vol. 15, no. 0, pp. 90–93, Aug. 2014.

[11] W. W. Yu, E. Chang, R. Drezek, and V. L. Colvin, "Water-soluble quantum dots for biomedical applications.," *Biochem. Biophys. Res. Commun.*, vol. 348, no. 3, pp. 781–6, Sep. 2006.

[12] R. Paper, L. Saravanan, S. Diwakar, R. Mohankumar, A. Pandurangan, and R. Jayavel, "Synthesis , Structural and Optical Properties of PVP Encapsulated CdS Nanoparticles," vol. 1, no. 2, pp. 42–48, 2011.

[13] S. K. Mishra, R. K. Srivastava, S. G. Prakash, R. S. Yadav, and a. C. Panday, "Structural, optical and photoconductivity characteristics of manganese doped cadmium sulfide nanoparticles synthesized by co-precipitation method," *J. Alloys Compd.*, vol. 513, pp. 118–124, Feb. 2012.

[14] P. Reyes and S. Velumani, "Structural and optical characterization of mechanochemically synthesized copper doped CdS nanopowders," *Mater. Sci. Eng. B*, vol. 177, no. 16, pp. 1452–1459, Sep. 2012.

[15] K.K. Nanda, S.N. Sahu: One-Dimensional Quantum Confinement in Electrodeposited PbS Nanocrystalline Semiconductors, Adv. Mater., 13 (2001) 280.

[16] Wang X, Zhuang J, Peng Q, Li Y: A general strategy for nanocrystal synthesis. Nature 2005, 437:121–124

[17] Bandaranayake R J,Wen GW, Lin J Y, Jiang H K and Sorensen: Structural phase behavior in II–VI semiconductor nanoparticles, CM1995 Appl. Phys. Lett. 67 831

[18] H.K. Yadav, K. Sreenivas, R.S. Katiyar, V. Gupta: Defect induced activation of Raman silent modes in rf co-sputtered Mn doped ZnO thin films, J. Phys. D: Appl. Phys. 40 (2007) 6005

[19] Alivisatos A P 1996 J. Phys. Chem. 100 13 226

[20] S. V. Gaponenko, optical properties of semiconductor nano crystals ,Cambridge university press ,1998.

[21] A. Henglein small particle research: physicchemical properties of extremely small colloid metal and semiconductor particles. Chem. Rev. 89, 1989, 1861-73

[22] P. V. Kamat, Photochemistry on nonreactive (semiconductor) surface, Chem. Rev. 93, 1993: 267-300.